Laser-Induced Spatial Symmetry Breaking in Quantum and Classical Mechanics

Ignacio Franco and Paul Brumer
Chemical Physics Theory Group, Department of Chemistry, and Center for Quantum Information and Quantum Control, University of Toronto, Toronto, Ontario, M5S 3H6, Canada
(Received 5 April 2006; published 28 July 2006)

Phase-controllable transport in laser-irradiated spatially symmetric systems is shown to arise both quantum mechanically and classically from a common field-driven interference mechanism. Specifically, the quantum-to-classical transition for symmetry breaking in a quartic oscillator driven by an $\omega + 2\omega$ field is studied. For this, a double perturbation theory in the oscillator anharmonicity and external field strength, that admits an analytic classical limit, is carried out in the Heisenberg picture. The interferences responsible for the symmetry breaking are shown to survive in the classical limit and are the origins of classical control. Differences between reflection symmetry that plays a key role in the analysis, and parity that does not, are discussed.

DOI: 10.1103/PhysRevLett.97.040402 PACS numbers: 03.65.−w

There are several qualitatively different ways to induce directed charge transport in spatially symmetric systems. The obvious choice is to subject the system to a bias voltage. Alternatively, it is also possible to drive the system with a zero-mean time-periodic electric field (e.g., a laser source) with frequency components $j\omega$ and $k\omega$, where j and k are integers of different parity. The response of the system is net dipoles or currents whose magnitude and sign can be manipulated by varying the relative phase between the two laser frequencies. Hence, the $j\omega + k\omega$ field breaks the inherent left/right symmetry of the system without introducing a bias in the potential. Below we focus on the popular case of $j = 1$, $k = 2$, although the arguments are quite general.

Laser-induced symmetry breaking has been studied theoretically [1–5] and demonstrated experimentally [6–8] in systems ranging from atoms to solid state samples. The effect is of general applicability and, with current laser technology, can be used to induce directed transport on a femtosecond time scale in any anharmonic symmetric system. Such field-induced asymmetry in quantum mechanics is attributed [1–3,8] to the creation of superposition states that are not eigenstates of the parity operator. Further, the quantum picture regards the symmetry breaking as arising from interference between two independent optical pathways to the same final state [1–3,7,8], an effect that is also nonclassical. Specifically, the two pathways in this case are a one-photon and a two-photon route. Since the one-photon process creates states with opposite parity to the initial state while the two-photon process couples states with the same parity, the interference between them creates an excited state of broken symmetry.

However, symmetry breaking has also been observed in classical mechanics [9], where parity is not a conserved quantity and quantum interference does not play a role. Further, unrelated classical and quantum arguments for symmetry breaking have been given in terms of the third-order nonlinear response of the system to the radiation field [10–12]. In this order, the system response mixes the laser frequencies and their harmonics in such a way as to generate a phase-controllable zero-harmonic (dc) component in the photoinduced dipoles/currents.

Given this collection of results it is, quite simply, unclear how quantum and classical symmetry breaking are related, if at all.

In this Letter we address this issue by analytically considering the quantum-to-classical transition of the net dipole induced by an $\omega + 2\omega$ field in a quartic oscillator. This is the simplest model with well-defined classical analog wherein induced symmetry breaking is manifest. To do so, we introduce a time-dependent perturbation theory approach in the Heisenberg representation that admits an analytic classical ($\hbar = 0$) limit [13] in the response of the oscillator to the field.

In addition to the actual result on symmetry breaking, the approach below significantly extends recent developments in perturbative studies in the Heisenberg picture [14,15] by (a) including the effects of the external field in the perturbative expansion, and (b) in establishing the power of the method in studies of classical-quantum correspondence. Further, by working in the Heisenberg picture we construct a useful time-dependent perturbation theory that is general and independent of the initial state. Although individual terms in the resultant quantum expression are found to have a singular classical limit, the overall result is shown to have an analytic $\hbar = 0$ limit that coincides with true classical behavior. In this way, it provides direct insight into symmetry breaking arising classically and quantum mechanically. Since physical insight is the primary focus of this work, resultant complicated analytic formulas are relegated to supplementary information [16].

Consider then a charged particle confined in a bounding quartic potential that is being driven by an external radiation field $E(t)$ in the dipole approximation. The anharmonic oscillator is defined by the Hamiltonian

$$H_0(x, p) = \frac{p^2}{2m} + \frac{1}{2}m\omega_0^2 x^2 + \lambda m\epsilon x^4, \qquad (1)$$

where x, p, and m denote the coordinate, momenta, and mass of the particle. Here $\lambda \in \{0, 1\}$, $\epsilon > 0$, with λ determining the strength of the anharmonicities in the potential. The total system Hamiltonian is

$$H(x, p, t) = H_0(x, p) - qxE(t), \qquad (2)$$

where q is the charge on the system and $E(t) = \epsilon_\omega \cos(\omega t + \phi_\omega) + \epsilon_{2\omega}\cos(2\omega t + \phi_{2\omega})$.

Insight into spatial asymmetry induced by $E(t)$ can be obtained via the long-time average of the position operator in Heisenberg picture, i.e., $\overline{\hat{x}_{\rm H}(t)}$, a quantity which measures the average symmetry breaking. To obtain this quantity we perform a double perturbative expansion for the operator $\hat{x}_{\rm H}(t)$ in the anharmonicities and in the radiation-matter interaction. The anharmonicities are included to minimal order in a multiple-scale approximation, while the interaction with the radiation field is taken into account up to third order.

Given $\hat{x}_{\rm H}(t)$, the classical solution $x(t)$ can then be extracted by first identifying the position and momentum operators, $\hat{x} = \hat{x}_{\rm H}(0)$ and $\hat{p} = \hat{p}_{\rm H}(0)$, in $\hat{x}_{\rm H}(t)$ with the classical position and momentum variables, $x = x(0)$ and $p = p(0)$, and then taking the limit $\hbar \to 0$, i.e.,

$$\hat{x}_{\rm H}(\hat{x}, \hat{p}, t) \xrightarrow[\hbar\to 0]{\hat{x}\to x, \hat{p}\to p} x[x(0), p(0), t]. \qquad (3)$$

With $\hat{x}_{\rm H}(t)$ and $x(t)$ one can then calculate quantum or classical averages for any initial state,

$$\langle\hat{x}\rangle(t) = {\rm Tr}[\hat{x}_{\rm H}(t)\hat{\rho}_0], \qquad \langle x\rangle_c(t) = {\rm Tr}[x(t)\rho_0(x, p)], \quad (4)$$

respectively. Here, $\hat{\rho}_0$ is the density matrix of the quantum system at preparation time, while $\rho_0(x, p)$ is a classical phase-space distribution of initial conditions.

Consider then the evolution operator $\hat{U}(t)$, which provides $\hat{x}_{\rm H}(t) = \hat{U}^\dagger(t)\hat{x}\hat{U}(t)$. A perturbative expansion of $\hat{U}(t)$ is most conveniently carried out in the interaction picture. In it, $\hat{U}(t) = \hat{U}_0(t)\hat{U}_{\rm I}(t)$, where $\hat{U}_0(t) = \exp(-\frac{i}{\hbar}\hat{H}_0 t)$ is the evolution operator in the absence of the field while $\hat{U}_{\rm I}(t)$ captures the effects induced by $\hat{V}(t) = -q\hat{x}E(t)$ on the dynamics. In this way the problem is split into two steps—a perturbative analysis to include the oscillator anharmonicity and a subsequent perturbation to include the external field. The former utilizes a recently obtained exact operator solution for $\hat{x}_{\rm I}(t) = \hat{U}_0^\dagger(t)\hat{x}\hat{U}_0(t)$ to minimal order in a quantum multiple-scale perturbation theory [15]. This solution includes corrections to all orders in the anharmonicities and, in this way, captures an additional time scale in the dynamics (the quantum analog of a first-order frequency shift). Reexpressed in terms of raising ($\hat{a}^\dagger$) and lowering ($\hat{a}$) operators and modified to adopt the units in the Hamiltonian [Eq. (1)], it reads

$$\hat{x}_{\rm I}(t) = x_0(e^{i(\omega_0+\hat{\delta}^-)t}\hat{a}^\dagger + e^{-i(\omega_0+\hat{\delta}^+)t}\hat{a}). \qquad (5)$$

Here, $\hat{\delta}^n = (\hat{\mathcal{H}} + n\hbar\omega_0/2)\xi$ is an operator that contains the renormalization of ω_0 due to the anharmonicities, $\xi = 3\epsilon\lambda/(m\omega_0^3)$ is proportional to the strength of the anharmonicities, $\hat{\mathcal{H}}(\hat{x}, \hat{p}) = \frac{\hat{p}^2}{2m} + \frac{1}{2}m\omega_0^2\hat{x}^2$ is the Harmonic oscillator Hamiltonian operator, $\hat{x} = x_0(\hat{a}^\dagger + \hat{a})$ and $\hat{p} = im\omega_0 x_0(\hat{a}^\dagger - \hat{a})$ are the position and momentum operators in the Schrödinger picture, and $x_0 = \sqrt{\hbar/(2m\omega_0)}$ is a characteristic length. In deriving Eq. (5) from the one in Ref. [15], it is useful to note that

$$\begin{aligned} \hat{a}f(\hat{\mathcal{H}} + k) &= f(\hat{\mathcal{H}} + \hbar\omega_0 + k)\hat{a}, \\ \hat{a}^\dagger f(\hat{\mathcal{H}} + k) &= f(\hat{\mathcal{H}} - \hbar\omega_0 + k)\hat{a}^\dagger; \end{aligned} \qquad (6)$$

for any operator $f(\hat{\mathcal{H}} + k) = \sum_{n=0}^\infty(\hat{\mathcal{H}} + k)^n f_n$, where f_n and k are c numbers. This follows from the commutation relations between $\hat{a}$ and $\hat{a}^\dagger$, $[\hat{a}, \hat{a}^\dagger] = \hat{1}$.

The perturbative expansion for $\hat{U}_{\rm I}(t)$ is given by [17] $\hat{U}_{\rm I}(t) = \hat{U}_{\rm I}^{(0)} + \hat{U}_{\rm I}^{(1)}(t) + \hat{U}_{\rm I}^{(2)}(t) + \hat{U}_{\rm I}^{(3)}(t) + \cdots$, where $\hat{U}_{\rm I}^{(0)} = \hat{1}$ is the zeroth-order term and

$$\hat{U}_{\rm I}^{(n)}(t) = -\frac{i}{\hbar}\int_0^t {\rm d}t'\hat{V}_{\rm I}(t')\hat{U}_{\rm I}^{(n-1)}(t') \qquad (n \geq 1), \quad (7)$$

the nth order correction. Here, $\hat{V}_{\rm I}(t) = -q\hat{x}_{\rm I}(t)E(t)$ is the radiation-matter interaction in the interaction picture. In order to solve Eq. (7) it is necessary to guarantee that all the operators within the integral commute; the required operator reordering was done using Eq. (6). Within this framework, $\hat{x}_{\rm H}(t) = \hat{U}_{\rm I}^\dagger(t)\hat{x}_{\rm I}(t)\hat{U}_{\rm I}(t)$ was calculated up to third order in the field. The result (where H.c. stands for Hermitian conjugate),

$$\begin{aligned} \hat{x}_{\rm H}(t) = \hat{x}_{\rm I} + [\hat{U}_{\rm I}^{(0)\dagger}\hat{x}_{\rm I}(\hat{U}_{\rm I}^{(1)} + \hat{U}_{\rm I}^{(2)} + \hat{U}_{\rm I}^{(3)}) + \tfrac{1}{2}\hat{U}_{\rm I}^{(1)\dagger}\hat{x}_{\rm I}\hat{U}_{\rm I}^{(1)} \\ + \hat{U}_{\rm I}^{(1)\dagger}\hat{x}_{\rm I}\hat{U}_{\rm I}^{(2)} + {\rm H.c.}], \end{aligned} \qquad (8)$$

is composed of 34 370 oscillatory terms that evolve on various time scales determined by the different combinations of the natural oscillator frequencies and the two laser frequencies. Out of all of them, only that subset that has a zero-frequency (dc) component in the oscillatory exponentials contributes to the net dipole. The remaining terms, with a residual frequency dependence, average out to zero in time. For example, all terms that are first order in the field average out to zero, so that symmetry breaking is a nonlinear optical effect.

Not all the dc terms in Eq. (8) induce symmetry breaking. If the initial state is symmetric, only those terms for which $i + j$ is odd in $\hat{U}_{\rm I}^{(i)\dagger}\hat{x}_{\rm I}(t)\hat{U}_{\rm I}^{(j)}$ give a nonzero contribution to the expectation value. That is, symmetry breaking comes from the interference between an even and an odd order response to the field. This result is well known when the initial state is a parity eigenstate [1–3,7]. However, in fact this result arises from considerations of reflection symmetry, rather than of conservation of parity, a subtle but significant distinction since parity is nonclassical.

To make explicit the distinction between being reflection symmetric and being in a state of definite parity, consider the density operator in the position representation: $\rho(x', x) = \langle x'|\hat{\rho}|x\rangle$. If $\rho(x', x) = \rho(-x', -x)$ the state is said to be reflection symmetric. Note that the Wigner distribution associated with such state will satisfy $\rho_W(x, p) = \rho_W(-x, -p)$, the usual statement of reflection symmetry. If, in addition, all the contributing states in the general mixture $\hat{\rho} = \sum_i p_i |\Psi_i\rangle\langle\Psi_i|$ are of the same parity then $\rho(x', x) = \pm\rho(x', -x) = \pm\rho(-x', x)$ and $\hat{\rho}$ is of definite parity. The latter two properties are a consequence of parity only and not of reflection symmetry. Being in a state of definite parity always implies reflection symmetry, but the converse is only true for pure states.

Consider then the role of reflection in determining the response to the field. Specifically, consider $\langle\hat{x}^n\hat{p}^m\rangle = \int dx dx' \langle x|\hat{x}^n\hat{p}^m|x'\rangle\rho(x', x) = (2\pi\hbar)^{-1}\int dx dx' dp x^n p^m \times e^{i(x-x')p/\hbar}\rho(x', x)$. If $\rho(x', x) = \rho(-x', -x)$ then $\langle\hat{x}^n\hat{p}^m\rangle = (-1)^{n+m}\langle\hat{x}^n\hat{p}^m\rangle$. Hence, only those terms with $(n+m)$ even make a nonzero contribution to the trace. In Eq. (8), this only happens for those terms with $(i+j)$ odd in $\hat{U}_I^{(i)\dagger}\hat{x}_I(t)\hat{U}_I^{(j)}$ because they have $\hat{a}^n\hat{a}^{\dagger m}$ with $(n+m)$ even, where $\hat{a} = (\hat{x} + i\hat{p}/m\omega_0)/(2x_0)$. As a result, the zeroth and second-order terms in Eq. (8) do not contribute to the expectation value and can be discarded. Parity considerations that solely arise in quantum mechanics do not, however, add anything to the analysis.

This approach yields a final operator expression for the net dipole:

$$\overline{\hat{x}_H(t)} = \overline{\hat{x}_I(t)\hat{U}_I^{(3)}(t)} + \overline{\hat{U}_I^{(1)\dagger}(t)\hat{x}_I(t)\hat{U}_I^{(2)}(t)} + \text{H.c.},$$
$$= \frac{q^3\epsilon_\omega^2\epsilon_{2\omega}}{16m^2\omega_0}\hat{\Gamma}(\hat{\mathcal{H}}, \omega, \lambda, \hbar)\cos(2\phi_\omega - \phi_{2\omega}), \qquad (9)$$

where the overbar denotes time averaging. The explicit expression for the operator $\hat{\Gamma}$ is given in the supplementary material [16]. Note that the only operator entering into $\hat{\Gamma}$ is $\hat{\mathcal{H}}$, i.e., $\hat{\Gamma}(\hat{\mathcal{H}}, \omega, \lambda, \hbar) = \sum_{n=0}^{\infty}\Gamma_n(\omega, \lambda, \hbar)\hat{\mathcal{H}}^n$, where the Γ_n coefficients are c numbers. Further, in the limit of zero anharmonicity, all symmetry breaking effects are lost, i.e. $\lim_{\lambda\to 0}\hat{\Gamma}(\hat{\mathcal{H}}, \omega, \lambda, \hbar) = 0$. Hence, it is precisely because of the anharmonicities that the system can exhibit a nonlinear response to the laser, mix the frequencies of the field and generate a zero-harmonic component in the response.

Equation (9) makes clear, first and foremost that the sign and magnitude of the dipole can be manipulated by varying the relative phase between the two frequency components of the laser. This central feature arises irrespective of the initial state and it is the source of control in laser-induced symmetry breaking. Further, the $\hbar \to 0$ limit of Eq. (9) is analytic and nonzero, despite the fact that individual perturbative terms entering into Eq. (9) can exhibit singular behavior as $\hbar \to 0$. Hence, the field-induced interferences responsible for symmetry breaking do not disappear in the classical limit and are the source of classical control.

A comparison of the classical solution

$$\overline{x(t)} = \frac{q^3\epsilon_\omega^2\epsilon_{2\omega}}{16m^2\omega_0}\Gamma_c(\mathcal{H}, \omega, \lambda)\cos(2\phi_\omega - \phi_{2\omega}) \qquad (10)$$

extracted from $\overline{\hat{x}_H(t)}$ as in Eq. (3) [where $\Gamma_c(\mathcal{H}, \omega, \lambda)$ is given in the supplementary material [16]] with a separate fully classical calculation, shows excellent agreement. For example, Fig. 1 shows a comparison of $\overline{x(t)}$ with a numerical integration of Newton's equations for a particle initially at rest ($\mathcal{H} = 0$). The two coincide for a wide range of anharmonicities and field strengths, the agreement being excellent for weak fields and small anharmonicities where the perturbative considerations are valid. Thus, we are able to recover true classical symmetry breaking from the quantum solution. Hence, the quantum and classical versions of laser control of symmetry breaking are one and the same physical phenomenon.

In the quantum case, the net dipoles can be divided into an $\hbar$-independent classical-like contribution $\overline{\hat{x}_c(t)} = \lim_{\hbar\to 0}\overline{\hat{x}_H(t)}$ and an entirely quantum-mechanical part $\overline{\hat{x}_q(t)}$, so that:

$$\overline{\hat{x}_H(t)} = \overline{\hat{x}_c(t)} + \overline{\hat{x}_q(t)}. \qquad (11)$$

The nature of the quantum corrections in this equation can be associated with the $\hbar$ dependence of the resonance structure of the oscillator. Indeed, within the approximations that underlie Eq. (9), the $\omega + 2\omega$ laser samples a total of eight resonances at $\{\frac{1}{2}[\omega_0 + (\hat{\mathcal{H}} \pm \hbar\omega_0/2)\xi]$, $\omega_0 + (\hat{\mathcal{H}} \pm \hbar\omega_0/2)\xi$, $\omega_0 + (\hat{\mathcal{H}} \pm \hbar\omega_0)\xi$, $2[\omega_0 + (\hat{\mathcal{H}} \pm \hbar\omega_0)\xi]\}$. As $\hbar \to 0$ these eight resonances merge together into three broad classical resonances at $[\frac{1}{2}(\omega_0 + \xi\hat{\mathcal{H}})$, $\omega_0 + \xi\hat{\mathcal{H}}$, $2(\omega_0 + \xi\hat{\mathcal{H}})]$ changing, in this way, the magnitude and sometimes the sign of symmetry breaking. For small anharmonicities the quantum character of the resonances is not apparent and $\overline{\hat{x}_H(t)} = \overline{\hat{x}_c(t)}$. In fact, quantum corrections only begin to appear at third order in λ.

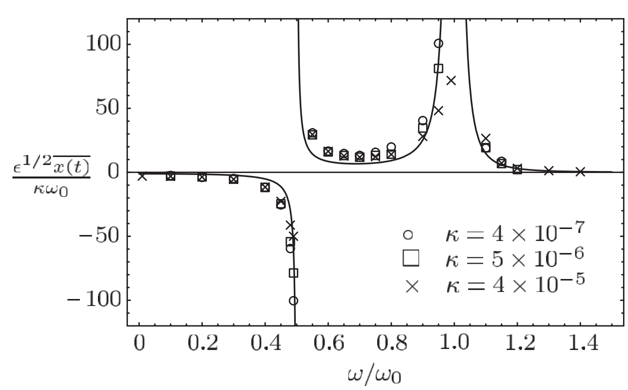

FIG. 1. Comparison of the classical limit of $\overline{\hat{x}_H(t)}$, $\overline{x(t)}$ (solid line), with the numerical solution (points) of Newton's equations, with $2\phi_\omega - \phi_{2\omega} = 0$ and $\mathcal{H} = 0$. Here $\kappa = q^3\epsilon_\omega^2\epsilon_{2\omega}\lambda\epsilon^{3/2}/(m^3\omega_0^9)$ is a quantifier of the strength of the field and the anharmonicities.

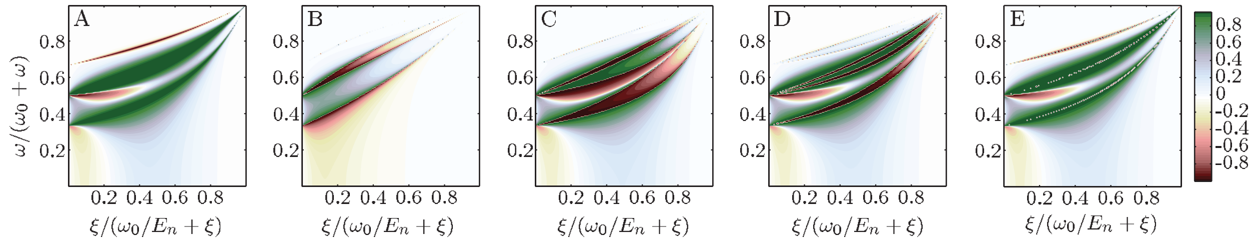

FIG. 2 (color). Net dipole induced by an $\omega + 2\omega$ field in a quantum and classical anharmonic oscillator. The contour plots show the dependence of $\frac{2}{\pi}\arctan[(16m^2\omega_0^4 E_n/[q^3\epsilon_\omega^2\epsilon_{2\omega}\cos(2\phi_\omega - \phi_{2\omega})])\langle\overline{\hat{x}_{\rm H}(t)}\rangle]$ on the anharmonicities of the potential (x axis) and the frequency of the field (y axis). The system is initially prepared in the nth eigenstate of $\hat{\mathcal{H}}$ with energy $E_n = \hbar\omega_0(n+\frac{1}{2})$. Panel (a) shows the classical part of the solution which in this parameter space is the same for all E_n. The remaining panels show the full quantum-mechanical solution for: (b) $n = 0$; (c) $n = 1$; (d) $n = 3$; and (e) $n = 40$. The color code is given at the far right.

Interestingly, when expectation values are calculated, as in Eq. (4), different initial states emphasize either $\overline{\hat{x}_c(t)}$ or $\overline{\hat{x}_q(t)}$ depending on the nature of the state. To demonstrate this and expose the differences between quantum and classical symmetry breaking, we explore the whole parameter space of Eqs. (9) and (10). To do so we are required to select an initial state. In the quantum case, we choose the nth eigenstate of $\hat{\mathcal{H}}$ with energy $E_n = \hbar\omega_0(n+\frac{1}{2})$. In the classical case, we choose a classical ensemble of particles with phase-space density $\rho_0(x,p) = \delta(\mathcal{H} - E_n)/\Omega$, where Ω is a normalization factor. For this density the classical ensemble average of $\overline{x(t)}$ coincides with the expectation value of the classical part of $\overline{\hat{x}_{\rm H}}$, $\langle\overline{x(t)}\rangle_c = \langle\overline{\hat{x}_c(t)}\rangle$. This is true because $\langle\Gamma_c(\mathcal{H},\omega,\lambda)\rangle_c = \Gamma_c(E_n,\omega,\lambda)$ in close analogy with the quantum case.

Figure 2 shows some representative results. The classical solution [Fig. 2(a)], which in the parameter space shown is the same for all E_n, is composed of three broad resonances at $\omega = [\frac{1}{2}(\omega_0 + \xi E_n), \omega_0 + \xi E_n, 2(\omega_0 + \xi E_n)]$. In contrast, the quantum solutions exhibit a fine $\hbar$-dependent resonance structure, making quantum symmetry breaking look very different from the classical one. For example, the quantum $n = 0$ case [Fig. 2(b)] differs dramatically from the classical solution except at small values for the anharmonicities. In all other cases, out of resonance and at small anharmonicities the classical and quantum solutions resemble one another. The situation is very different near resonances where the quantum features can be dominant. Nevertheless, as the energy E_n of the initial state increases [the progression shown in Figs. 2(b)–2(e)], and becomes large with respect to $\hbar\omega_0$, the quantum resonances gradually merge together into three broad classical resonances. That is, the state progressively emphasizes the classical part of $\overline{\hat{x}_{\rm H}(t)}$, $\overline{\hat{x}_c(t)}$, and quantum and classical symmetry breaking coincide.

In conclusion, we have shown that laser control of symmetry breaking in quantum and classical systems correspond to the same physical phenomenon, with a common reliance on classically meaningful reflection symmetry arguments, rather than parity. The observed symmetry breaking is a consequence of field-driven interferences that do not vanish in the classical limit.

This work was supported by NSERC Canada. We thank Dr. Jiangbin Gong for discussions on an earlier version of this manuscript.

[1] M. Shapiro and P. Brumer, *Principles of the Quantum Control of Molecular Processes* (Wiley-Interscience, New York, 2003).
[2] G. Kurizki, M. Shapiro, and P. Brumer, Phys. Rev. B **39**, 3435 (1989).
[3] R. Atanasov *et al.*, Phys. Rev. Lett. **76**, 1703 (1996).
[4] E. J. Mele, P. Král, and D. Tománek, Phys. Rev. B **61**, 7669 (2000).
[5] K. A. Pronin and A. D. Bandrauk, Phys. Rev. B **69**, 195308 (2004).
[6] Y. Y. Yin *et al.*, Phys. Rev. Lett. **69**, 2353 (1992).
[7] E. Dupont *et al.*, Phys. Rev. Lett. **74**, 3596 (1995).
[8] A. Haché *et al.*, Phys. Rev. Lett. **78**, 306 (1997).
[9] S. Flach, O. Yevtushenko, and Y. Zolotaryuk, Phys. Rev. Lett. **84**, 2358 (2000); M. Porto, M. Urbakh, and J. Klafter, *ibid.* **85**, 491 (2000); S. Denisov, J. Klafter, and M. Urbakh, Phys. Rev. E **66**, 046203 (2002); J. Gong and P. Brumer, *ibid.* **70**, 016202 (2004); R. D. Astumian and P. Hänggi, Phys. Today **55**, No. 11, 33 (2002).
[10] N. B. Baranova, A. N. Chudinov, and B. Y. Zel'dovich, Opt. Commun. **79**, 116 (1990).
[11] I. Goychuk and P. Hänggi, Europhys. Lett. **43**, 503 (1998).
[12] S. Denisov *et al.*, Phys. Rev. E **66**, 041104 (2002).
[13] T. A. Osborn and F. H. Molzahn, Ann. Phys. (N.Y.) **241**, 79 (1995).
[14] G. Auberson and M. C. Peyranère, Phys. Rev. A **65**, 032120 (2002); S. Banerjee and J. K. Bhattacharjee, Phys. Rev. Lett. **93**, 120403 (2004).
[15] C. M. Bender and L. M. A. Bettencourt, Phys. Rev. Lett. **77**, 4114 (1996); Phys. Rev. D **54**, 7710 (1996).
[16] See EPAPS Document No. E-PRLTAO-97-033631 for the expression for $\hat{\Gamma}$ and Γ_c. For more information on EPAPS, see http://www.aip.org/pubservs/epaps.html.
[17] A. L. Fetter and J. D. Walecka, *Quantum Theory of Many-Particle Systems* (Dover, New York, 2003).